# Constantly renewing glacial lakes in the Kyrgyz Range, northern Tien Shan

Mirlan Daiyrov[1], Chiyuki Narama[2]

[1]Graduate School of Science and Technology, Niigata University, Niigata city, 950-2181, Japan
[2]Program of Field Research in the Environmental Sciences, Niigata University, Niigata city, 950-2181, Japan

*Correspondence to*: Mirlan Daiyrov (mirlan085@gmail.com)

**Abstract.** In the Kyrgyz Range of the northern Tien Shan, Central Asia, glacial lakes have been a focus of monitoring due to the increasing concern over glacial lake outburst floods (GLOFs) amid notable glacier recession. This study investigates (1) the historical evolution in numbers and area of glacial lakes (each>0.00045 km²) for the period 1968, 2000, and 2021, using Corona KH-4, Landsat 7, and Sentinel-2 imagery, and (2) the relationship between lake development and the evolution of glacier-moraine complexes (GMCs) containing buried ice. The number of glacial lakes doubled between 1968 and 2021, while the total area increased by 76% (0.80 to 1.42 km²). However, 190 out of 274 lakes present in 1968 had disappeared by 2000. Many new lakes emerged by 2021, with one lake reappearing after a prior disappearance since 1968. Rapid lake formation was associated with a 32% reduction in glacier area over the past 50 years and the evolution of GMCs. The expansion and melt of buried ice of IDCs led to new surface depressions (thermokarst features) and subsequent lake formation, resulting in continuous glacial lake renewal. Thus, the continuous renewal of glacial lakes in the Kyrgyz Range results from the combined effects of glacier retreat, GMC expansion, and buried ice melt.

## 1 Introduction

It has been reported that the number of glacial lakes in high mountain regions of Asia is rapidly increasing (Zhang et al., 2023). In the Kyrgyz Range located in the northern Tien Shan of Kyrgyz Republic, hundreds of glacial lakes are identified by satellite data (Kattel et al., 2020; Daiyrov et al., 2022). Development of these lakes predominantly occurs on glacier moraine complexes (GMCs, Shatravin, 2007; Erokhin, 2011), which formed during glacier retreat after the Little Ice Age (LIA). GMCs is also referred to as the ice-debris complex (Bolch et al., 2018; Blöthe et al., 2021). A GMC is a geomorphological unit that combines buried glacier ice with moraine deposits. Post-Little Ice Age climatic warming induced geomorphological transformations of these moraine deposits, with buried ice becoming trapped under debris during glacier recession (Maksimov, 1982; Maksimov and Osmonov, 1995; Erokhin et al., 2017). As buried ice melted, numerous glacial lakes formed on GMCs, sometimes in direct contact with their parent glaciers, but often as independent thermokarst lakes (Janský et al., 2008). Lakes directly connected to glacier terminus typically exhibit faster expansion due to glacier recession,

though indirectly connected lakes can also enlarge through debris-covered ice melt (Daiyrov et al., 2018; 2022). Approximately 20% of these lakes are considered potentially hazardous (Janský et al., 2008, 2010).

Monitoring glacial lakes in the Kyrgyz Range is critical, as repeated GLOFs have caused severe damage (Erokhin et al., 2008, 2017; Kattel et al., 2020). Systematic research began in the 1960s following catastrophic GLOF events in Kyrgyzstan. In the central part of Kyrgyz Range, at least 22 GLOF events have been recorded since 1952 (Erokhin, 2011; Zaginaev et al., 2016), including recent floods and debris flow such as Takyrtor glacial lake on 5 June 2009, Teztor glacial lake on 31 July 2012, Chelektor glacial lake on 12 August 2017, Akpai glacial lake on 2 August 2021 (Erokhin et al., 2017; Kattel et al., 2020; Daiyrov et al., 2022), and Takyrtor glacial lake on 27 June 2025. These events damaged infrastructure, agricultural fields, and downstream settlements (Erokhin et al., 2017; Zaginaev et al., 2019), demonstrating the need for ongoing hazard assessment (Kattel et al., 2020; Daiyrov et al., 2022). Compared to the eastern Himalayas, where the glacial lakes have been expanding continuously for decades (Yamada et al., 1998; Komori et al., 2004; Nagai et al., 2017), glacial lakes in the northern Tien Shan including the Kyrgyz Range are smaller and more susceptible to unstable, short-term fluctuations due to geomorphological conditions, such as drainage of ice tunnel within GMCs (Daiyrov et al., 2018; Narama et al., 2018). Despite often being small, these lakes can pose significant hazards, especially since these lakes described as "short-lived" (Narama et al., 2010, 2018; Daiyrov et al., 2018, 2022; Daiyrov and Narama, 2021) or "non-stationary" (Erokhin et al., 2017) lakes may form and drain in rapid succession, sometimes producing catastrophic GLOFs.

The increase in glacial lakes has been reported across High Mountain Asia (HMA). However, the processes of glacial lake formation and the factors behind GLOFs vary greatly from region to region. To accurately understand the relationship between glacial lake development and GLOFs, it is essential to understand the distinctive features of each locality. In the Kyrgyz Range, Central Asia, previous studies documented lake numbers and area (Shatravin and Stavisski, 1984; Jansky et al., 2006; Usubaliev and Erokhin, 2007; Erokhin, 2008; Falatkova et al., 2019; Daiyrov et al., 2022). Despite observations of the number and area of glacial lakes, long-term changes in glacial lakes and the processes driving lake renewal in this region remain insufficiently documented. To understand the characteristics of formation history in glacial lakes and to clarify the processes of rapid glacial lake renewal in the Kyrgyz Range, this study investigates (1) the historical evolution in numbers and area of glacial lakes during 1968, 2000, and 2021, based on Corona KH-4, Landsat 7/ETM+, and Sentinel-2 imagery, and (2) the relationship between lake development and the evolution of glacier-moraine complexes (GMCs) containing buried ice. The latter relationship was investigated through analysis of glacier area change due to various remote sensing imagery and d elevation models (DEMs) for the study.

## 2 Study area

The study area is the Kyrgyz Range in the northern Tien Shan (Fig. 1), with mountain ridges ranging from 2,500 to 4,900 m above sea level. The central northern flank, has many glaciers, is higher than the eastern and western flanks. Post-glacier retreat GMCs consisting of dead ice and debris are widely distributed at glacier fronts (Shatravin, 2007). These GMCs are

distinct from debris-covered glaciers, and the lakes forming on them are typically small, non-stationary, and thermokarst type, although some are connected by internal drainage channels, leading to GLOFs (Narama et al., 2018). Some GMC termini have evolved into glacier-derived rock glaciers. Climate change over recent decades has driven glacier and GMC shrinkage and degradation (Erokhin et al., 2017; Daiyrov et al., 2022).

In total, 483 glaciers covering approximately 520 km² between 3,100 and 4,200 m elevation have been identified (Usubaliev et al., 2013), concentrated mostly in central river basins including Issyk-Ata, Alamudun, West-Karakol, and Sokuluk (Maksimov and Osmonov, 1995). The Ala-Archa basin glacier area decreased by 15.2–18% between 1963/64 and 2003–2010 (Aizen et al., 2006; Bolch, 2015). The Golubin Glacier (5.42 km²) is the largest in the Kyrgyz Range, with a long-term mass balance averaging −0.20 ± 0.42 m w.e./year from 1949/50 to 2020/21 (Azisov et al., 2022). The largest GMC (~3 km²) is located at the Ken-Tor glacier front in the Noruz River basin (Maksimov and Osmonov, 1995).

Precipitation peaks between March and July, with an average annual precipitation of 787 mm and mean annual temperature of −3.5°C (1969-2005) at the Teo-Ashuu meteorological station (3,400 m) in the central range. Precipitation is a critical factor influencing glacier mass balance (Ponomarenko, 1976; Aizen et al., 2006).

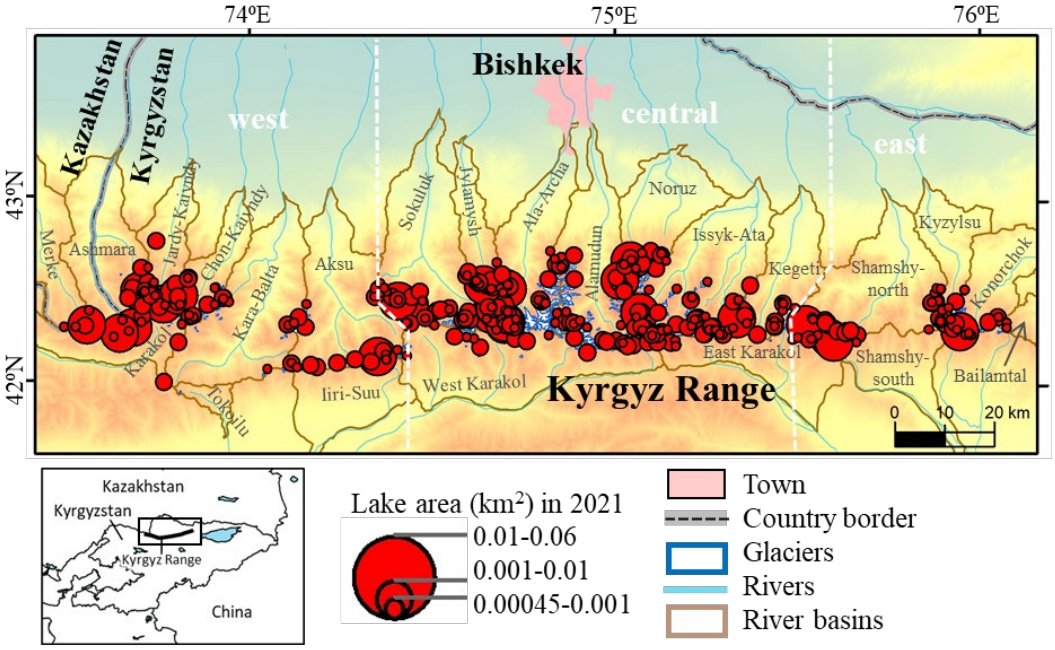


**Figure 1: Maps of the study area in the Kyrgyz Range, northern Tien Shan. The top map shows the Kyrgyz Range, with glacial lakes in 2021 marked by red circles. The bottom left map highlights study sites in Kyrgyzstan. The Kyrgyz Range is divided into three sections by white dotted lines. Glacial lake sizes correspond to circle diameters.**

## 3 Methods

### 3.1 Satellite data collection

To quantify the historical changes in glacial lakes and glaciers within the Kyrgyz Range, we utilized a combination of satellite remote sensing datasets spanning five decades using Corona, Landsat 7/ETM+ and Sentinel-2. Thirteen near cloud-free Corona KH-4 stereo photographs from 1964 and 1968 formed the earliest dataset, covering 2% (predominantly 14 glaciers on the eastern part) and 98% of the study region, respectively. Each image spans ~16 km in width with a spatial resolution between 1.8 and 2.7 meters (Table 1). DEMs and orthoimages were generated from forward and aft stereo-image pairs using Metashape (Agisoft), with geometric distortions corrected via a non-metric camera model. Ground control points (GCPs) for geometric correction were systematically chosen from stable terrain features such as large boulders outside glacier and GMC areas. Coordinates were derived from Google Earth's QuickBird images and advanced land observing satellite/panchromatic remote sensing instrument for stereo mapping (ALOS/PRISM) ortho images (2.5 m resolution) dated 2007, while vertical references originated from HMA DEM data (8 m resolution) from 2017. Each stereo pair processing employed 25–30 GCPs segmented into four area groups (a–d), carefully excluding cloudy or snow-covered features to preserve accuracy. The final Corona-derived DEM and orthophotos achieved 4.1 m and 2.0 m spatial resolutions, respectively. We also used orthoimages of Landsat 7/ETM+ in 2000 (15 m) and Sentinel-2 (10 m) in 2021 (Table 2). We used Landsat 7 pan-sharpened images converted from 15 m panchromatic (8 band) and 30 m multispectral images using ArcGIS Pro. These scenes without significant cloud or snow contamination were used from analysis to maintain data quality and reliability.

**Table 1: List of Corona KH-4 images of the study area.**

| Satellite | Corona Scenes | Date | Ground resolution (m) | Coverage area in study area (%) |
|---|---|---|---|---|
| KH-4A 10 (Corona 85, Mission 1010, OPS 3497) | DS1010-2086DA121<br>DS1010-2086DA120<br>DS1010-2086DF114<br>DS1010-2086DF115 | 20.09.1964 | 2.7 | east part : 2% |
| KH-4A 48 (Corona 128, Mission 1048, OPS 0165) | DS1048-1039DA030<br>DS1048-1039DA031<br>DS1048-1039DA032<br>DS1048-1039DF030<br>DS1048-1039DF031<br>DS1048-1039DF032 | 18.09.1968 | 2.7-7.6 | west, central and east part: 74% |
| KH-4B 4 (Corona 127, Mission 1104, OPS 5955) | DS1104-2185DF053<br>DS1104-2185DA057<br>DS1104-2185DA058 | 07.08.1968 | 1.8 | central-south and east part: 24% |

### 3.2 Mapping of glacial lakes, glaciers, and GMCs

To understand the changes of the areas and numbers of glacial lakes since 1960s, we manually digitized glacial lakes from Corona KH-4 images (1964, 1968), Landsat 7/ETM+ (2000), and Sentinel-2 (2021) using ArcGIS Pro (Table 2). Manual mapping ensures higher delineation accuracy compared to semi-automated methods, though boundary uncertainties persist at pixel-level interfaces between water and land. Unclear outline of lakes due to shadow in the Corona imagery were assessed using slope data from Corona DEM; regions with less than 10°slope in uncertain zones were cautiously included as lake area if visually plausible, otherwise excluded to prevent overestimation. Snow-covered and cloud-covered areas did not affect lake mapping, as they were areas without glacial lakes.

We implemented a series of pre-processing steps in ArcGIS Pro to ensure both spatial and spectral consistency between Landsat 7 and Sentinel-2 images. For stable land areas, we verified that pixel values from the two sensors were comparable and that normalized difference vegetation index (NDVI) values indicated similar vegetation cover. These checks confirmed that the datasets could be reliably compared for subsequent analysis.

For image composition, we selected Landsat 7 bands 1, 2, and 3 to create an RGB composite suitable for water feature delineation, and mapped lake outlines from Sentinel-2 imagery (10 m resolution) using corresponding bands 1, 2, and 3. To maintain consistency in glacial lake detection across the multitemporal imagery, we set a minimum mapping threshold of 0.00045 km², equivalent to two pixels of 15-m Landsat image. This threshold was uniformly applied to Corona, Landsat, and Sentinel-2 datasets, thus permitting temporal comparisons of lake area change. After manual delineation of lake boundaries, we calculated lake parameters and classified them as either contactless or glacier-contact types. Area changes for individual lakes were quantified for the years 1968, 2000, and 2021, and shifts in lake type composition over time were also assessed.

Although manual mapping of lake polygons yields higher accuracy than semi-automated techniques, it is subject to image quality limitations such as boundary ambiguity at lake margins (Hanshaw and Bookhagen, 2014). This arises because pure water pixels often adjoin mixed pixels containing both water and land, making precise classification of edge pixels challenging. To account for these uncertainties, we followed the method of Hanshaw and Bookhagen (2014) to estimate area error, and excluded lakes with ambiguous boundaries from our analysis. To further assess sensor-related uncertainty, we selected a stable reference lake outside the GMC zone, clearly visible in all image types. Manual delineation using consistent NDWI thresholds enabled direct comparison of mapped lake areas across sensors. The analysis showed that Landsat 7 produced slightly larger lake area estimates than the 1968 reference (absolute difference: 0.000326 km²; relative difference: 8.8%), whereas Sentinel-2 (2021) provided results closer to the baseline (absolute difference: 0.000127 km²; relative difference: 3.4%). The superior spatial resolution of Sentinel-2 contributed to a more precise delineation. Nevertheless, an 8.8% uncertainty margin is generally acceptable for glacial lake mapping when using Landsat data and manual mapping. Consequently, we adopted this reference lake for estimating overall sensor-related uncertainty. The consistency of these findings with our previous work in the Kyrgyz Range (Daiyrov et al., 2022) further validates the approach.

Glaciers were manually mapped using Corona KH-4 imagery from 1964 and 1968, as well as Sentinel-2 imagery from 2021. Only images acquired under minimal cloud and snow cover were selected for analysis to ensure accurate boundary identification. All Corona images from 1968 and Sentinel-2 scenes from 2021 were captured during the summer months (August for Sentinel-2, August and September for Corona), minimizing seasonal snow effects (Table 1). Glacier boundaries were delineated by visual interpretation of standard false color composites constructed from multi-spectral imagery. Glacier area changes between 1964/1968 and 2021 were then quantitatively calculated based on these polygonal outlines.

**Table 2: List of Satellite images for glacial lake extraction.**

| Satellite | Sensor | Date | Ground resolution (m) | ID: |
|---|---|---|---|---|
| Landsat 7 | Enhanced Thematic Mapper (ETM) | 07.07.2000 | 30 | LE07_L1TP_151031_20000707_20200918_02_T1 |
| | | 07.07.2000 | 30 | LE07_L1TP_151030_20000707_20200918_02_T1 |
| | | 16.07.2000 | 30 | LE07_L1TP_150030_20000716_20200918_02_T1 |
| | | 16.07.2000 | 30 | LE07_L1TP_150031_20000716_20200918_02_T1 |
| | | 30.07.2000 | 30 | LE07_L1TP_152031_20000730_20200917_02_T1 |
| | | 30.07.2000 | 30 | LE07_L1TP_152030_20000730_20200918_02_T1 |
| | | 24.08.2000 | 30 | LE07_L1TP_151031_20000824_20200918_02_T1 |
| | | 24.08.2000 | 30 | LE07_L1TP_151030_20000824_20200917_02_T1 |
| | | 02.09.2000 | 30 | LE07_L1TP_150031_20000902_20200917_02_T1 |
| | | 02.09.2000 | 30 | LE07_L1TP_150030_20000902_20200918_02_T1 |
| Senitnel-2 | Multi-Spectral Instrument (MSI) | 24.07.2021 | 10 | S2A_MSIL2A_20210724T054641_N0500_R048_T43TEH_20230220T005731.SAFE |
| | | 11.08.2021 | 10 | S2B_MSIL2A_20210811T055639_N0500_R091_T43TCH_20230215T033526.SAFE |
| | | 11.08.2021 | 10 | S2B_MSIL2A_20210811T055639_N0500_R091_T43TCG_20230215T033526.SAFE |
| | | 11.08.2021 | 10 | S2B_MSIL2A_20210811T055639_N0500_R091_T43TDH_20230215T033526.SAFE |
| | | 11.08.2021 | 10 | S2B_MSIL2A_20210811T055639_N0500_R091_T43TDG_20230215T033526.SAFE |
| | | 11.08.2021 | 10 | S2B_MSIL2A_20210811T055639_N0500_R091_T43TEH_20230215T033526.SAFE |
| | | 21.08.2021 | 10 | S2B_MSIL2A_20210821T055639_N0500_R091_T43TCH_20230210T193704.SAFE |
| | | 21.08.2021 | 10 | S2B_MSIL2A_20210821T055639_N0500_R091_T43TCG_20230210T193704.SAFE |
| | | 21.08.2021 | 10 | S2B_MSIL2A_20210821T055639_N0500_R091_T43TDH_20230210T193704.SAFE |
| | | 21.08.2021 | 10 | S2B_MSIL2A_20210821T055639_N0500_R091_T43TDG_20230210T193704.SAFE |
| | | 21.08.2021 | 10 | S2B_MSIL2A_20210821T055639_N0500_R091_T43TEH_20230210T193704.SAFE |
| | | 05.09.2021 | 10 | S2A_MSIL2A_20210905T055641_N0500_R091_T43TCG_20230118T130151.SAFE |
| | | 05.09.2021 | 10 | S2A_MSIL2A_20210905T055641_N0500_R091_T43TEH_20230118T130151.SAFE |
| | | 07.09.2021 | 10 | S2B_MSIL2A_20210907T054639_N0500_R048_T43TEH_20230118T203059.SAFE |
| | | 27.09.2021 | 10 | S2B_MSIL2A_20210927T054639_N0500_R048_T43TEH_20230124T140016.SAFE |

To map GMCs in the study area, we employed several geomorphological criteria. GMCs were identified as continuous, debris-covered surfaces up to 3 km in length extending from the glacier front, lacking prominent moraine ridges, and exhibiting a convex cross-sectional profile. The absence of continuous valley-bottom drainage channels was confirmed through interpretation of Google Earth imagery. We also assessed the presence of preserved ice within GMCs using differential interferometric SAR (DInSAR) analysis to detect surface deformation. These GMCs developed during glacier retreat since the Little Ice Age and typically comprise various moraine landforms and buried ice (Shatravin, 2007; Erokhin, 2011). GMCs were delineated according to these geomorphological characteristics and boundaries established in previous

regional studies (Maksimov, 1982; Maksimov and Osmonov, 1995; Shatravin and Stavisski, 1984; Shatravin, 2007; Erokhin, 2008, 2011). GMC boundaries were manually digitized using Sentinel-2 imagery from 2021; where image clarity was insufficient, higher-resolution Corona KH-4 images from 1964 and 1968 were referenced to refine the delineations. All area mapping utilized false color multi-spectral composite imagery acquired under conditions with minimal cloud and snow cover.

### 3.3 Geomorphological analysis using DInSAR

To quantify the number of GMCs containing buried ice, we conducted DInSAR analysis using GAMMA SAR software and ALOS/Phase Array type L-band Synthetic Aperture Radar (PALSAR) and ALOS-2/PALSAR-2 (L-band) datasets. GMCs exhibiting surface displacement—identified as coherent displacement fringes representing both horizontal and vertical ground movements—were interpreted as likely containing significant ice content. Displacement fringes, revealed in the DInSAR results, indicate active surface processes such as permafrost creep or the subsidence resulting from the melting of buried ice. The technical approach and interpretation follow established methodologies detailed in previous works (Goldstein et al., 1997; Werner et al., 2001; Quincey et al., 2007; Sandwell et al., 2008; Daiyrov et al., 2018).

Our analysis employed both long-interval (>10 months, spanning winter) and short-interval (1–3 months, summer) image pairs, comprising 49 images (18 from ALOS/PALSAR, 2009–2010; 31 from ALOS-2/PALSAR-2, 2014–2016), all with perpendicular baselines less than 1,500 m. Table 3 provides a part of list of image pairs used. The DInSAR processing workflow consisted of converting raw SAR data to Single Look Complex (SLC) format, coregistering SLCs, generating differential interferograms, removing topographic phase using Shuttle Radar Topography Mission (SRTM) DEM, unwrapping interferometric phase to obtain displacement information, and geocoding results into a geographic coordinate system. Noise from temporal and spatial decorrelation was suppressed using an adaptive filter (Goldstein et al., 1997; Goldstein and Werner, 1998). In our results, displacement fringes in long-interval pairs primarily record slow subsidence, while those in short-interval pairs reveal more rapid surface motion. This distinction follows earlier findings, such as those for the Swiss Alps' Gruben rock glacier, where only short-interval interferograms successfully detected surface motion (Strozzi et al., 2004).

To verify buried ice within GMCs based on DInSAR, we compared surface motion signals at the Chelektor Glacier front with known ice occurrences, and found that internal ice consistently corresponded with DInSAR-detected displacement. Additional ground truthing was performed using GNSS measurements at the Adygine Glacier GMC, further supporting the interpretation. The presence of ice in GMCs has also been confirmed in the Teskey Range of the northern Tien Shan by both DInSAR and field surveys (Daiyrov et al., 2018). Areas of pronounced deformation were also analyzed using DEM differencing (HMA, 2017 and UAV, 2018), which indicated substantial surface changes coincident with mapped buried ice. Thus, DInSAR-detected deformation in moraine complexes is interpreted as evidence of ice-rich conditions, with melt-induced subsidence as the probable mechanism (Daiyrov et al., 2018).

**Table 3: List of ALOS data (a part of data).**

| Pair | Master ID | Slave ID | Master Date (YYYYMMDD) | Slave Date (YYYYMMDD) | Span (days) | Bperp (m) | Orbit | Offnadir angle(°) |
|---|---|---|---|---|---|---|---|---|
| A | ALOS2015180840-140903 | ALOS2058650840-150624 | 20140903 | 20150624 | 294 | 100.4 | Ascending | 36.2 |
| B | ALPSRP239030840 | ALPSRP245740840 | 20100720 | 20100904 | 46 | 337 | Ascending | 34.3 |
| C | ALPSRP079740840 | ALPSRP240780840 | 20070724 | 20100801 | 1104 | 1332.7 | Ascending | 34.3 |
| D | ALOS2064120840-150731 | ALOS2074470840-151009 | 20150731 | 20151009 | 70 | 90.9 | Ascending | 32.5 |
| E | ALOS2018580840-140926 | ALOS2072400840-150925 | 20140926 | 20150925 | 364 | -14.2 | Ascending | 28.2 |
| F | ALPSRP236550840 | ALPSRP243260840 | 20100703 | 20100818 | 46 | 143.3 | Ascending | 34.3 |

### 3.4 Geomorphological analysis using DEMs and their accuracy assessment

Widespread formation of surface depression (thermokarst feature) on glacier and GMC is attributed to surface subsidence caused by melting buried ice (Erokhin et al., 2017; Narama et al., 2010, 2018; Daiyrov et al., 2018; Daiyrov and Narama, 2021). To investigate the long-term morphological changes of GMCs, we compared Corona in 1968 and HMA DEMs. In addition, to investigate morphological changes of GMC, field surveys using unmanned aerial vehicles (UAVs) were conducted for GMC in Chelektor Glacier, central Kyrgyz Range in summers of 2018 (15 July) and 2023 (28 July), generating complementary high-resolution data. The 2018 campaign mapped the entire GMC, whereas 2023 coverage was partial due to unfavorable weather, focusing primarily on the glacier terminus. The Phantom4 RTK platform (DJI) captured geotagged imagery processed in Pix4Dmapper to yield orthoimages at 5.4 m and DEM at 1.0 m resolution. Finally, the amount of vertical decline was calculated by comparing Corona (4.1 m resolution, 1968), SRTM (30 m, 2000), HMA (8 m, 2017), and UAV DEMs (1.0 m, 2018 and 2023). Surface depression polygons for 1968, 2000, 2017, 2018, and 2023 were generated using a hydrologic 'filling' algorithm in ArcGIS Pro to quantitatively assess area changes over time.

The vertical accuracy of these datasets was evaluated against HMA DEM, which provides an accurate, temporally consistent terrain reference. Stable terrain areas devoid of glacier and GMC were selected as benchmarks. Elevation data from the Corona, SRTM, and UAV DEMs were aligned to HMA reference elevations to correct systematic vertical offsets. Subsequently, elevation differences of the corrected DEMs were computed within polygon area around stable points. The Root Mean Square Error (RMSE) values were within acceptable ranges for geomorphological analysis: 2.2 m for Corona DEM, 2.8 m for SRTM, and 1.3 m for UAV. These error margins are appropriate considering the study scale and the terrain's elevation gradients, although Corona's limited GCP density and SRTM's coarse resolution limit their ultimate vertical fidelity.

## 4 Results

### 4.1 Changes in glacial lake numbers and areas during 1968–2021

We identified 274 glacial lakes in 1968, 380 lakes in 2000, and 412 lakes by 2021 (Fig. 2), demonstrating that the total number of glacial lakes in the Kyrgyz Range effectively doubled over the study period. Of the original 274 lakes present in

1968, 190 (69%) had disappeared by 2000. Similarly, of the 380 lakes observed in 2000, 142 had disappeared by 2021. In contrast, 84 lakes have persisted from 1968 through 2021. Substantial renewal occurred, with 154 new lakes (41% of the total in 2000) and 175 new lakes (42% of the total in 2021) observed in each subsequent time step. Notably, one lake that had vanished by 2000 reappeared by 2021 (Fig. 2). The high rate of both lake disappearance and new formation suggests a dynamic process of glacial lake renewal, which contrasts the more gradual and continual expansion of glacial lakes observed in the eastern Himalayas since the mid-twentieth century (Yamada, 1998; Ageta et al., 2000; Iwata et al., 2002; Komori et al., 2004). This study used >0.1 km2 threshold and they got 773 lakes. By contrast, there is no lakes of >0.1km2 in our study area. We changed sentence.This pattern of rapid lake formation and loss is consistent with trends reported for the Kungoy and Ili Ranges, also within the northern Tien Shan (Narama et al., 2009).

Figure 3 illustrates the distribution of lakes by size class over time. In 1968, small lakes (0.00045–0.001 km²) comprised 36% of all glacial lakes, while by 2000 and 2021, this proportion had decreased to 18–22%. Medium-sized lakes (0.001–0.01 km²) dominated the area spectrum, accounting for 60% of total lake area in 1968, rising to 78% in 2000 and 71% in 2021. The number of large lakes (0.01–0.1 km²) increased from 11 in 1968 to 30 in 2021, and the total area of these lakes expanded 2.6-fold, from 0.23 km² to 0.59 km². A total of 773 glacial lakes larger than 0.1 km² have been identified in the Bhutan Himalayas (Nagai et al., 2017), whereas no glacial lakes exceeding 0.1 km² are present in the Kyrgyz Range.

The cumulative glacial lake area increased from 0.80 km² in 1968 to 1.20 km² in 2000, and by 2021, the area had increased by an additional 18% to reach 1.42 km². Among the 84 lakes that persisted for the entire study period, area changes were significant: 14 exhibited substantial variability, with changes ranging from 0.005 to 0.053 km² between 1968 and 2021. Of the lakes present in 2000, 152 experienced areal variation, including 13 with marked increases (0.005–0.053 km²) between 2000 and 2021. Spatial analysis further shows that the largest lakes predominantly formed at the termini of retreating glaciers, while most medium and small lakes developed on GMCs farther from active glacier ice.

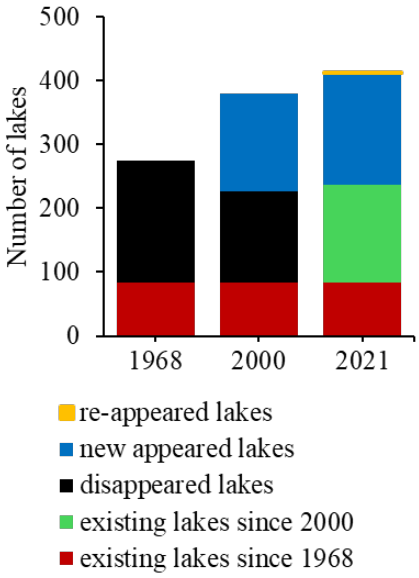


230

**Fig. 2. Numbers of glacial lakes and their changes in 1968, 2000 and 2021.**

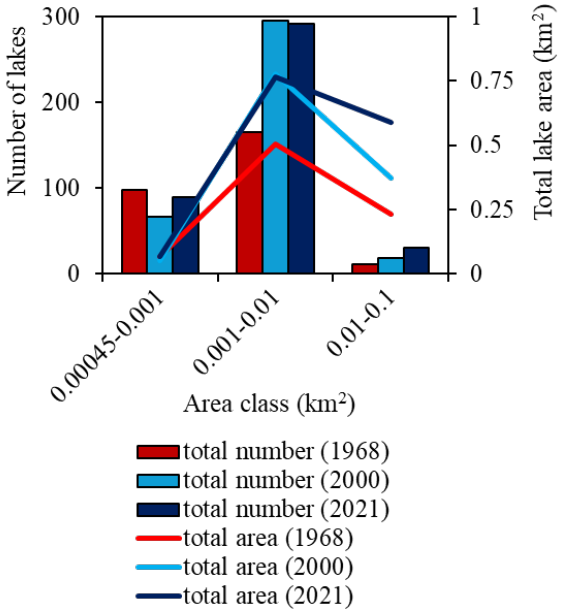


**Figure 3: Numbers and areas of glacial lakes in the three area classes in 1968, 2000 and 2021.**

## 4.2 Types of glacial lakes and their evolution

In this region, glacial lakes were classified into two principal types based on their spatial relationship to glaciers: glacier-contact (proglacial) lakes and contactless (thermokarst) lakes (Fig. 4a). The classification was determined solely by the current location of each lake relative to the glacier margin, rather than differences in genesis. Glacier-contact lakes are situated adjacent to glacier termini and are typically impounded by GMC, moraines, or bedrock. In contrast, contactless lakes—primarily thermokarst in origin—form on the surface of GMCs as a result of the melting of buried glacier ice. Some thermokarst lakes exhibit pronounced seasonal variations in surface area, including phases of stability, expansion, contraction, emergence, disappearance, and short-lived existence—phenomena often observed in supraglacial lakes on debris-covered glaciers due to their connection with evolving drainage channels (Daiyrov et al., 2018). In addition, detailed classifications of the lakes in the study area can be found in previous reports (Erokhin, 2008, 2011; Janský et al., 2006, 2010).

Long-term analysis reveals a notable shift in lake types over time (Fig. 4b). While 45% (124 of 274) of the lakes identified in 1968 were contactless, this proportion rose to 72% (272 of 380) in 2000 and 71% (291 of 412) in 2021, indicating a significant increase in the number of thermokarst lakes on GMCs. Conversely, the number of glacier-contact lakes has steadily decreased since 1968. As illustrated in Fig 4c, the fate of individual lakes underscores these trends: of the 150 glacier-contact lakes present in 1968 (including one documented in 1964), only 26 remained classified as contact lakes by 2021, 36 had transitioned to contactless status due to glacier retreat, and 88 had disappeared altogether. Of the 124 contactless lakes identified in 1968, 55 persisted through 2021 while 70 ceased to exist.

These results highlight that, unlike the eastern Himalayas—where glacier-contact lakes can persist and expand over extended periods (Yamada, 1998; Nagai et al., 2017)—such lakes in the Kyrgyz Range tend to be transient. Here, rapid glacier retreat combined with generally steeper glacier-front slopes tends to separate former contact lakes from glacier termini, while limited development of large GMCs and flat outwash plains further impedes the sustained expansion and longevity of glacier-contact lakes (Agarwalet al., 2023).

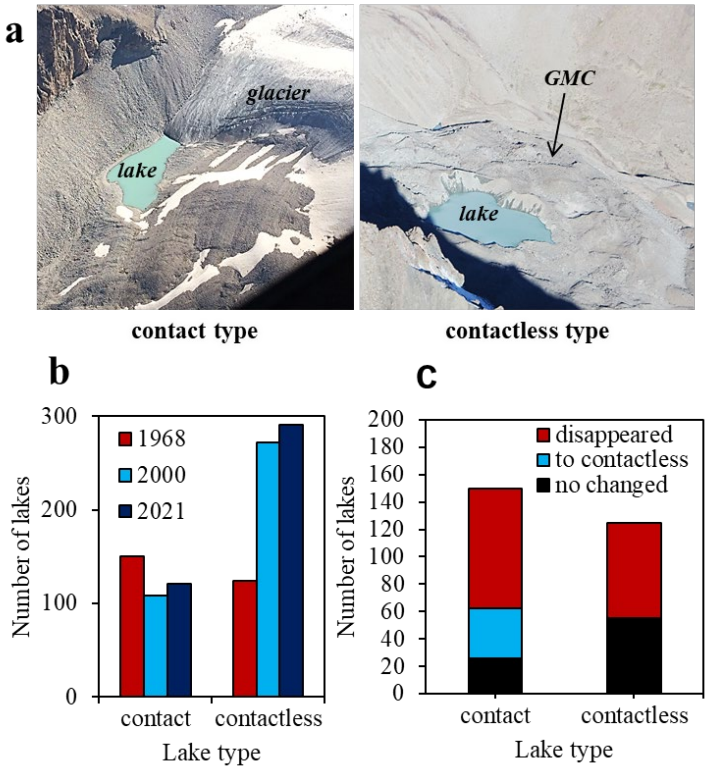


**Figure 4: a) Photographs of the two types of glacial lakes: glacier-contact (left); contactless (right) . b) Comparison of the number of glacial lakes by type in 1968, 2000, and 2021. c) Transitions in lake type from 1968 to 2021.**

### 4.3 Area changes in glaciers and surface changes in GMCs

To elucidate the processes underpinning the recent formation and disappearance of glacial lakes, we analyzed temporal changes in both glacier extent and glacier-moraine complexes (GMCs) across the Kyrgyz Range between 1968 and 2021. Substantial retreat of glacier termini occurred throughout this period, resulting in the transformation of recently deglaciated terrain into GMCs (Fig. 5a). The total glacier area decreased from 390.3 km² in 1968 to 265.4 km² in 2021, reflecting a reduction of 32% over 53 years (Fig. 5b). Spatially, 72% of the glacierized area was concentrated in the central Kyrgyz Range, while the western and eastern sectors accounted for 19% and 9%, respectively. The relative rates of glacier shrinkage were 30% in the central region, 36% in the west, and 40% in the east.

We identified 611 GMCs in the Kyrgyz Range. Focusing on GMCs—particularly those host to numerous contactless (thermokarst) lakes—our comparison of DEMs from Corona in 1968 and HMA in 2017 showed that 112 (18%) of the 611 GMCs in the Kyrgyz Range experienced substantial surface lowering of −5 to −30 meters. Extensive vertical declines (−10 to −30 m) were especially evident in GMCs within the Sokuluk, Jylamysh, Ala-Archa, Alamudun, Noruz, Issyk-Ata, and Kegeti river basins (Fig. 1). DInSAR data covering 2007–2010 and 2014–2016 further revealed that 450

(74%) of 611 GMCs underwent significant displacement, a signal that is consistent with surface adjustment attributable to the melting of buried ice (Fig. 5c; Daiyrov et al., 2018; Daiyrov and Narama, 2021). These DInSAR results also enabled identification of GMCs with strong potential for future lake formation.

At the Chelektor Glacier GMC—a representative site in the central range—three surface depressions (thermokarst feature) formed between 1968 and 2017 (Fig. 6a,b). Morphological evidence, such as imagery and DEM differences, clearly demonstrate that ice melt induced both surface subsidence and depression formation (Fig. 6c). From 2000 to 2021, depression-1 grew substantially (Fig. 6d); comparative photographs from 2015 and 2018 highlight these rapid changes (Fig. 7a,b). Over a three-year interval, the surface area of the depression nearly doubled. Elevation profiles (Fig. 7c,f) document a maximum surface lowering of −23 m for depression-1 and −28 m for depression-2, confirming significant geomorphic evolution. As Chelektor Glacier retreated, new glacial lakes formed within these depressions, illustrating the close linkage between glacier dynamics, GMC transformation, and lake development (Fig. 7d,e).

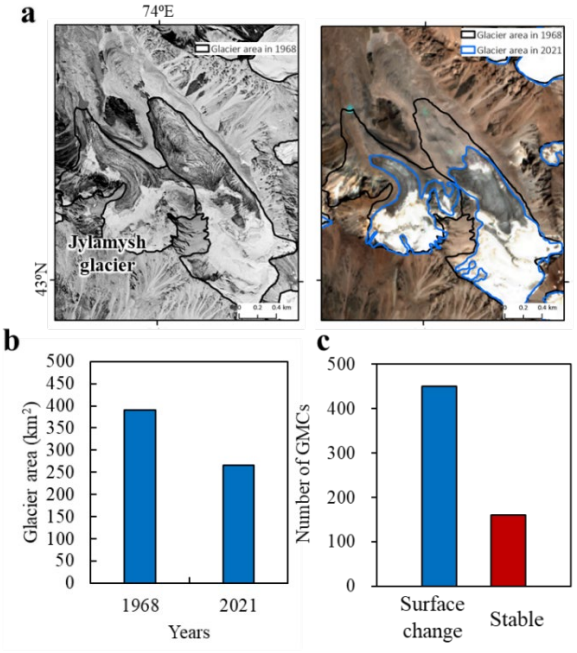


**Figure 5: a) Glacier shrinkage in the Kyrgyz Range, illustrated by satellite images from different years: Corona KH-4B (1968, left) and PlanetScope (2021, right). b) Changes in glacier area in the Kyrgyz Range between 1968 and 2021. c) Number of GMCs detected at the surface changes based on DInSAR data.**

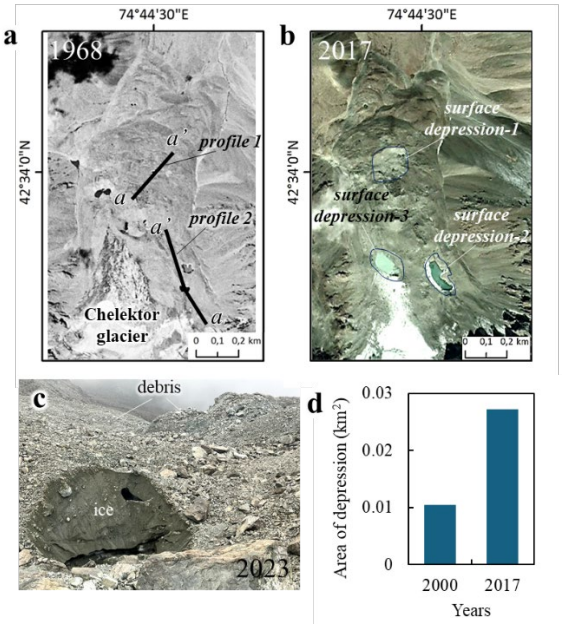


**Figure 6: a-b) Development of a surface depression on GMC at the Chelektor Glacier front (location in Fig. 1), illustrated by satellite images from different years: Corona KH-4B (1968, left) and PlanetScope (2017, right). c) Exposed ice on GMC. d) Area changes of surface depression-1 from 2000 to 2017.**

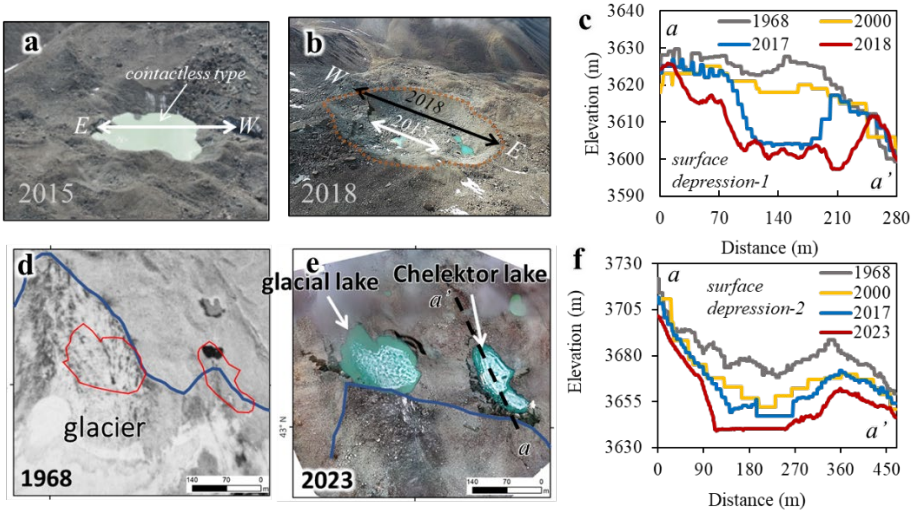


**Figure 7: Surface depression development and the formation of new glacial lakes on GMC at the Chelektor glacier front. a, b) Photographs of surface depression-1 in 2015 and 2018. c, f) Changes in surface depression profiles (profile lines indicated in Fig. 6a). d) Orthoimage from Corona (1968). e) UAV orthoimage from 2023. Profile data are derived from DEMs of 1968 (Corona), 2000 (SRTM 1), 2017 (High Mountain Asia), and 2018-2023 (UAV data).**

### 4.4 Differences in glacial lake patterns among river basins

Figure 8a summarizes the evolution of lake count, glacier loss, and GMC area for three sectors of the Kyrgyz Range, with boundaries shown in Fig. 1. While glacial lake numbers increased steadily in the western and central regions from 1968 to 2021, a slight decrease was recorded in the east. Notably, the highest concentration of glacial lakes and GMCs is found in the central range, where glacier loss has also been somewhat lower than in the peripheries. This pattern is likely a function of the central region's higher elevations and larger ice masses, both factors that confer greater resistance to melting and disintegration (Aizen et al., 1997, 2006). Nonetheless, both the western and eastern sectors have experienced the disappearance of many small glaciers (Aizen et al., 2006; Bolch et al., 2007).

When disaggregating by river basin (Fig. 8b), most glacial lakes are concentrated in the Issyk-Ata, Sokuluk, Alamudun, and Ala-Archa catchments in the central range. In contrast, the Shamshy-North basin in the east and Ak-Suu basin in the west are the only non-central basins with more than 30 lakes, while all other catchments have fewer than 30. Repeated development of new surface depressions in the central GMCs—particularly in the Sokuluk, Jylamysh, Ala-Archa, Alamudun, Noruz, and Issyk-Ata river basins—was associated with significant GMC surface changes. This highlights the central Kyrgyz Range as a key area for both rapid GMC evolution and ongoing glacial lake formation, particularly thermokarst types engendered by accelerated buried ice melt.

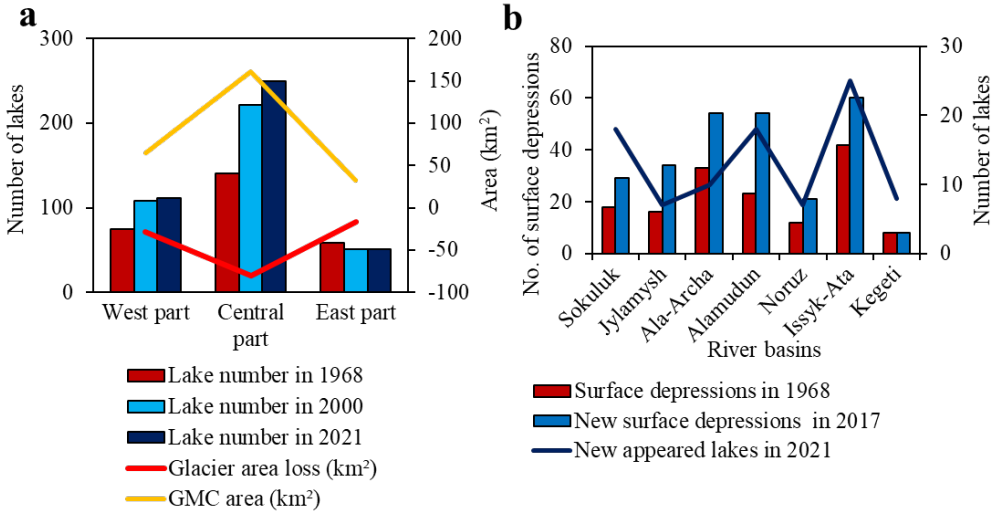


**Figure 8: a) Number of lakes in 1968, 2000, and 2021, and areas of glacier loss and GMCs in the three sections of the Kyrgyz Range. b) Number of surface depressions in 1968 and 2017, as well as new lakes formed between 2000 and 2021 in the central part of the range.**

## 5 Discussion

### 5.1 Mechanisms underlying rapid glacial lake renewal

Between 2000 and 2021, 42% of the glacial lakes in the Kyrgyz Range were newly formed (Fig. 2), highlighting an exceptionally dynamic system. This rapid turnover mirrors trends observed in the Kungoy and Ili Ranges of the northern Tien Shan (Narama et al., 2009). The dominant driver is glacier shrinkage—glacier area has decreased by approximately 30% over the past five decades. As glaciers retreat, large portions of their forefields become GMCs, leading to the expansion of potential sites for lake formation (Fig. 5a).

The accelerated formation of contactless (thermokarst) lakes is further supported by the observed expansion and deepening of surface depressions (thermokarst features), resulting from the melting of buried ice within GMCs. For example, at the Chelektor Glacier front, both downwasting and backwasting of buried ice resulted in substantial morphological changes and the lateral expansion of lake margins (Figs. 6, 7). This mirrors geomorphic processes observed on debris-covered glaciers elsewhere (Goldstein and Werner, 1997). Large depressions form as a result of glacier surface downwasting, as documented in the Teskey Range (Narama et al., 2010), filling with meltwater and transitioning into glacial lake.

Contrasting the eastern Himalayas, where glacier-contact lakes often persist and gradually expand for decades (Yamada, 1998; Ageta et al., 2000; Iwata et al., 2002; Komori et al., 2004; Nagai et al., 2017), glacier retreat in the Kyrgyz Range has mostly resulted in either the disappearance of contact lakes or their transformation into contactless types (Fig. 4c). Lakes formerly connected to glaciers become isolated as glaciers retreat upslope, no longer receiving direct meltwater input, which often results in their eventual disappearance. The persistence and reappearance of contactless lakes is linked to local geomorphological conditions, such as the existence of ice tunnels, buried ground ice, and the recurrent formation of surfaces depressions on GMC. When meltwater or stream channels intersect these depressions, new thermokarst lakes can form, sometimes repeatedly at the same location.

Recent climate warming has greatly enhanced the sensitivity of GMCs to melting, increasing rates of depression formation and thus enabling further glacial lake development (Daiyrov et al., 2018; Daiyrov and Narama, 2021). Given these processes, GMCs should be recognized as important environments driving the future proliferation of contactless glacial lakes in the region (Falatkova et al., 2019). Notably, in the Himalayas, lake development remains more directly linked to glacier shrinkage and the presence of large terminal moraines or flat outwash plains (Mool et al., 2001a; Iwata et al., 2002; Yamada, 1998). In contrast, the Kyrgyz Range setting, with steep glacier forefields and ice-cored moraines, promotes more rapid and recurrent short-lived lake development—a trend likely to accelerate further under continued warming and rising glacier equilibrium lines (Marchenko et al., 2007; Niederer et al., 2008). This highlights the strong influence of glacier retreat and subsequent GMC evolution on dynamics of glacial lake formation and persistence within the study region.

### 5.2 Regional variability in lake development

Glacial lake formation and turnover in the Kyrgyz Range exhibit pronounced spatial concentration in the central basins of Sokuluk, Ala-Archa, Alamudun, and Issyk-Ata, where the density and expansion of GMCs and rapid glacier shrinkage together foster exceptional rates of dynamic lake emergence and disappearance, and also increased hazard potential. This central zone has also experienced the majority of GLOF events over the past 20 years (Erokhin et al., 2017; Kattel et al., 2020; Daiyrov et al., 2022), most triggered by sudden drainage through ice tunnels within GMCs. Such processes are characterized by frequent depressions and subsequent thermokarst lake development, directly linked to ice-rich GMC morphology and the ablation of buried ice. Detailed DInSAR and UAV survey data corroborate this spatial variability, demonstrating that rapid surface lowering within central GMCs fosters recurrent cycles of lake creation. By contrast, peripheral river basins characterized by fewer or more stable GMCs have shown relatively limited changes in glacial lake systems.

Comparable findings have been reported nearby regions of the northern Tien Shan. In the Teskey Range, thermokarst lakes exhibit rapid fluctuations in surface area that are closely associated with GMC conditions (Daiyrov et al., 2018; Daiyrov and Narama, 2021). Short-term variavility in glacial lakes has been attributed to persistent ablation of buried ice, resulting in rapid transitions in lake type. Short-term lake variations caused variability in lake type, and many of them changed under GMC change. Among these lake types, short-lived type caused most recent GLOFs in the Kyrgyz and Teskey Ranges (Narama et al., 2010, 2018; Erokhin et al., 2017; Daiyrov et al., 2020, 2022). Among these, short-lived lakes have been responsible for most recent GLOFs in both the Kyrgyz and Teskey Ranges. The triggering mechanism for such events since 2000 has often been the temporary closure and reopening of ice tunnels within GMCs. Tunnel blockage may result from debris deposition or the freezing of water within ice tunnels (Erokhin et al., 2012; Narama et al., 2018), debris deposition is frequently linked to melting of dead ice within GMCs (Daiyrov et al., 2018; Daiyrov and Narama, 2021). The thawing of buried ice through thermokarst processes leads to surface subsidence, collapse, and the subsequent formation of distinctive thermokarst lakes (Kääb and Haeberli, 2001). Thus, lake development in the Teskey Range is strongly governed by GMC conditions and the presence of large volumes of buried ice.

Given the continued rise in regional temperatures, further melting of dead ice within GMCs is anticipated, likely resulting in additional depression enlargement, accelerated lake formation, and increased risk of sudden drainage events (GLOFs). Continuous monitoring and hazard assessment focused on GMC-rich areas—especially those with population centers downstream—are therefore critical, even as this study does not directly model future GLOF scenarios. Nonetheless, our documentation of buried-ice GMCs and rapidly evolving lakes offers an important foundation for anticipating and mitigating cryospheric hazards in the Kyrgyz Range.

At the broader High Mountain Asia (HMA) scale, lake expansion and GLOF hazards are increasingly recognized. Furian et al. (2022) projected the formation of large proglacial lakes across HMA through 2100. Recent studies demonstrated accelerated glacial lake growth and applied moraine-dam outburst models such as the eastern Himalayas for GLOF risk

assessment (Zhang et al., 2023; Chen et al., 2024). However, the processes of lake formation and GLOF triggering in the Tien Shan differ fundamentally from those in the eastern Himalayas. Therefore, effective assessment of disaster preparedness and future projections requires (1) current records of region-specific lake development and GLOF history, and (2) a detailed understanding of the characteristic lake formation processes specific to each mountain region.

## 6 Conclusions

This study quantifies the dynamic evolution of glacial lakes in the Kyrgyz Range, northern Tien Shan, over the period 1968–2021. During these 53 years, the number of glacial lakes increased from 274 in 1968 to 412 in 2021—a near doubling—while total lake area expanded by 76%, from 0.80 km² to 1.42 km². Turnover was extremely high: of the 274 lakes present in 1968, 190 (69%) had disappeared by 2000. Despite these losses, 154 new lakes appeared by 2000, and 175 more had formed by 2021, with just 84 lakes persisting across the entire study period. Glacier area shrank by 32%, from 390.3 km² to 265.4 km², driving widespread formation of glacier–moraine complexes (GMCs) rich in buried ice. Surface lowering of up to 5-30 m was observed in 18% of GMCs, and DInSAR analysis revealed that 74% of GMCs showed measurable deformation, promoting the rapid development of new, often thermokarst lakes. By 2021, over 70% of all glacial lakes were contactless types, reflecting the dominance of lake formation in GMCs over persistent proglacial expansion. These processes underpin a regime of constant glacial lake renewal, contrasting with the gradual expansion seen in the Himalayas.

In the Kyrgyz Range, glacial lakes renew rapidly due to the combination of accelerated glacier retreat, the expansion of glacier–moraine complexes (GMCs) containing buried ice, and ongoing climate warming. As glaciers shrink, newly exposed GMCs with significant dead ice melt and subside, forming new surface depressions that quickly fill with meltwater to create short-lived lakes. This geomorphological instability, coupled with repeated melting and reformation cycles, leads to a highly dynamic regime where glacial lakes frequently disappear, reappear, or form anew. The central Kyrgyz Range, particularly the Sokuluk, Ala-Archa, and Issyk-Ata basins where many glaciers and GMCs are distributed, remains a hotspot for lake turnover and associated hazards. As warming continues, monitoring lake dynamics and GMC changes will be vital for hazard assessment and adaptation in the region.

**Funding**

Grant-in-Aid for Scientific Research (B) (19H01372 and 23K22023) of MEXT KAKENHI Grant.

**Acknowledgments**

This work was supported by Grant-in-Aid for JSPS Fellows (22F22006) of JSPS KAKENHI Grant and Grant-in-Aid for Scientific Research (B) (19H01372 and 23K22023) of MEXT KAKENHI Grant. This study used ALOS satellite image data from ALOS Research Announcement (RA) in the framework of JAXA EORC.

**References**


Agarwal, V., Wyk de Vries, M. V., Haritashya, U. K., Garg, S., Kargel, J. S., Chen, Y., and Shugar, D. H.: Long-term analysis of glaciers and glacier lakes in the Central and Eastern Himalaya, Sci. Total Environ., 898, 165598, https://doi.org/10.1016/j.scitotenv.2023.165598, 2023.

Ageta, Y., Iwata, S., Yabuki, H., Naito, N., Sakai, A., Narama, C., and Karma.: Expansion of glacier lakes in recent decades in the Bhutan Himalayas, in: IAHS Publ., Wallingford, UK, 165–175, 2000.

Aizen, V. B., Aizen, E. M., and Melack, J. M.: Climate and hydrologic changes in the Tien Shan, central Asia, J. Climate, 10, 1393–1404, 1997.

Aizen, V. B., Kuzmichenok, V. A., Surazakov, A. B., and Aizen, E. M.: Glacier changes in the central and northern Tien Shan during the last 140 years based on surface and remote-sensing data, Ann. Glaciol., 43, 202–213, https://doi.org/10.3189/172756406781812465, 2006.

Azisov, E., Hoelzle, M., Vorogushyn, S., Saks, T., Usubaliev, R., Esenaman uulu, M., and Barandun, M.: Reconstructed centennial mass balance change for Golubin Glacier, northern Tien Shan, Atmosphere, 13, 954, https://doi.org/10.3390/atmos13060954, 2022.

Blöthe, J. H., Halla, C., Schwalbe, E., Bottegal, E., Liaudat, D. T., and Schrott, L.: Surface velocity fields of active rock glaciers and ice-debris complexes in the Central Andes of Argentina, Earth Surf. Process. Landf., 46, 504–522, https://doi.org/10.1002/esp.5042, 2021.

Bolch, T.: Climate change and glacier retreat in northern Tien Shan (Kazakhstan/Kyrgyzstan) using remote sensing data, Glob. Planet. Change, 56, 1–12, https://doi.org/10.1016/j.gloplacha.2006.07.009, 2007.

Bolch, T.: Glacier area and mass changes since 1964 in the Ala-Archa Valley, Kyrgyz Ala-Too, northern Tien-Shan, Ice Snow, 129, 28–39, https://doi.org/10.15356/IS.2015.01.03, 2015.

Bolch, T., Rohrbach, N., Kutuzov, S., Robson, B. A., and Osmonov, A.: Occurrence, evolution and ice content of ice-debris complexes in the Ak-Shiirak, Central Tien Shan revealed by geophysical and remotely-sensed investigations, Earth Surf. Process. Landf., 44, 129–143, https://doi.org/10.1002/esp.4487, 2019.

Chen, M., Chen, Y., Fang, G., Zheng, G., Li, Z., and Li, Y.: Risk assessment of glacial lake outburst flood in the Central Asian Tienshan Mountains, Clim. Atmos. Sci., 7, 209, https://doi.org/10.1038/s41612-024-00755-6, 2024.

Daiyrov, M., Narama, C., Yamanokuchi, T., Tadono, T., Kääb, A., and Ukita, J.: Regional geomorphological conditions related to recent changes of glacial lakes in the Issyk-Kul basin, northern Tien Shan, Geosciences, 8, 99, https://doi.org/10.3390/geosciences8030099, 2018.

Daiyrov, M., Narama, C., Kääb, A., and Tadono, T.: Formation and outburst of Toguz-Bulak glacial lake in the north part of Teskey Range, Tien Shan, Kyrgyzstan, Geosciences, 10, 468, https://doi.org/10.3390/geosciences10110468, 2020.

Daiyrov, M., Kattel, D. B., Narama, C., and Wang, W.: Evaluating the variability of glacial lakes in the Kyrgyz and Teskey Ranges, Tien Shan, Front. Earth Sci., 14, 112–119, 2022.

Daiyrov, M., and Narama, C.: Formation, evolution, and drainage of short-lived glacial lakes in permafrost environments of the northern Teskey Range, Central Asia, Nat. Hazards Earth Syst. Sci., 21, 2245–2256, https://doi.org/10.5194/nhess-21-2245-2021, 2021.

Erokhin, S.: Data report of glacial lakes in 2000–2008, in: Inventory of Glacial Lakes, Ministry of Emergency Situations of the Kyrgyz Republic, Bishkek, (in Russian), 2008.

Erokhin, S.: Types of moraine complexes and Tien-Shan glaciation, Izvestiya NAS KR, Bishkek, 115–118 (in Russian), 2011.

Erokhin, S., Zaginaev, V., Meleshko, A., Ruiz-Villanueva, V., Petrakov, D. A., and Chernomorets, S. S.: Debris flows triggered from nonstationary glacier lake outbursts: The case of the Teztor Lake complex (Northern Tian Shan, Kyrgyzstan), Landslides, 15, 83–98, https://doi.org/10.1007/s10346-017-0862-3, 2017.

Falatkova, K., Šobr, M., Neureiter, A., Schöner, W., Janský, B., Häusler, H., Engel, Z., and Beneš, V.: Development of proglacial lakes and evaluation of related outburst susceptibility at the Adygine ice-debris complex, northern Tien Shan, Earth Surf. Dynam., 7, 301–320, https://doi.org/10.5194/esurf-7-301-2019, 2019.

Furian, W., Maussion, F., and Schneider, C.: Projected 21st-century glacial lake evolution in high mountain Asia, Front. Earth Sci., 10, 821798, https://doi.org/10.3389/feart.2022.821798, 2022.

Goldstein, R. M., and Werner, C. L.: Radar ice motion interferometry, in: Proc. 3rd ERS ESA Symp., ESA SP, Florence, Italy, 969–972, 1997.

Goldstein, R. M., and Werner, C. L.: Radar interferogram phase filtering for geophysical applications, Geophys. Res. Lett., 25, 4035–4038, 1998.

Hanshaw, M. N., and Bookhagen, B.: Glacial areas, lake areas, and snow lines from 1975 to 2012: Status of the Cordillera Vilcanota, including the Quelccaya ice cap, northern central Andes, Peru, Cryosphere, 8, 359–376, https://doi.org/10.5194/tc-8-359-2014, 2014.

Iwata, S., Ageta, Y., Sakai, A., Narama, C., and Karma.: Glacial lakes and their outburst flood assessment in the Bhutan Himalaya, Glob. Environ. Res., 6, 3–17, 2002.

Janský, B., Šobr, M., and Erokhin, S. A.: Typology of high mountain lakes of Kyrgyzstan with regard to the risk of their rupture, Limnol. Rev., 6, 135–140, 2006.

Janský, B., Šobr, M., and Engel, Z., and Yerokhin, S.: High-altitude lake outburst: Tien-Shan case study, in: Dostál, P. (Ed.), Evolution of geographical systems and risk processes in the global context, Charles Univ. Prague, Faculty of Science, P3K Publishers, Prague, 113–127, 2008.

Janský, B., Šobr, M., and Engel, Z.: Outburst flood hazard: Case studies from the Tien-Shan Mountains, Kyrgyzstan, Limnol-Ecol. Manage. Inland Waters, 40, 358–364, 2010.

Kääb, A., and Haeberli, W.: Evolution of a high-mountain thermokarst lake in the Swiss Alps, Arct. Antarct. Alp. Res., 33, 385–390, https://doi.org/10.1080/15230430.2001.12003445, 2001.

Kattel, D. B., Mohanty, A., Daiyrov, M., Wang, W., Mishra, M., Kulenbekov, Z., and Dawadi, B.: Evaluation of glacial lakes and catastrophic floods on the northern slopes of the Kyrgyz Range, MRD, 40, 3, https://doi.org/10.1659/MRD-JOURNAL-D-19-00068.1, 2020.

Komori, J., Gurung, D. R., Iwata, S., and Yabuki, H.: Variation and lake expansion of Chubda Glacier, Bhutan Himalayas, during the last 35 years, Bull. Glaciol. Res., 21, 49–55, https://doi.org/10.5331/bgr.21.49, 2004.

Maksimov, E. V.: Climate Change and Mountain Glaciation in the New Era, Proc. Russian Geogr. Soc., 114, 2, 1982.

Maksimov, E. V., and Osmonov, A. O.: Features of modern glaciation and glacier dynamics of the Kyrgyz Ala-Too, Natl. Acad. Sci. Kyrgyz Rep., Tian Shan Phys.-Geogr. Stn. Inst. Geol., Bishkek, Ilim, 200 pp., ISBN 5-8355-0845-X, 1995.

Marchenko, S. S., Gorbunov, A. P., and Romanovsky, V. E.: Permafrost warming in the Tien Shan Mountains, Central Asia, Glob. Planet. Change, 56, 311–327, https://doi.org/10.1016/j.gloplacha.2006.07.023, 2007.

Mool, P. K., Bajracharya, S. R., and Joshi, S. P.: Inventory of Glaciers, Glacial Lakes and Glacial Lake Outburst Floods, Monitoring and Early Warning Systems in the Hindu Kush-Himalayan Region: Nepal, ICIMOD & UNEP RRC-AP, 2001.

Nagai, H., Ukita, J., Narama, C., Fujita, K., Sakai, A., and Tadono, T.: Evaluating the scale and potential of GLOF in the Bhutan Himalayas using a satellite-based integral glacier-glacial lake inventory, Geosciences, 7, 77, https://doi.org/10.3390/geosciences7030077, 2017.

Narama, C., Severskiy, I., and Yegorov, A.: Current state of glacier changes, glacial lakes, and outburst floods in the Ile Ala-Tau and Kungöy Ala-Too ranges, northern Tien Shan Mountains, Ann. Hokkaido Geogr., 84, 22–32, https://doi.org/10.14943/geoexp.84.22, 2009.

Narama, C., Duishonakunov, M., Kääb, A., Daiyrov, M., and Abdrakhmatov, K.: The 24 July 2008 outburst flood at the western Zyndan glacier lake and recent regional changes in glacier lakes of the Teskey Ala-Too range, Tien Shan, Kyrgyzstan, Nat. Hazards Earth Syst. Sci., 10, 647–659, https://doi.org/10.5194/nhess-10-647-2010, 2010.

Narama, C., Daiyrov, M., Duishonakunov, M., Tadono, T., Sato, H., Kääb, A., Ukita, J., and Abdrakhmatov, K.: Large drainages from short-lived glacial lakes in the Teskey Range, Tien Shan Mountains, Central Asia, Nat. Hazards Earth Syst. Sci., 18, 983–995, https://doi.org/10.5194/nhess-18-983-2018, 2018.

Niederer, P., Bilenko, V., Ershova, N., Hurni, H., Yerokhin, S., and Maselli, D.: Tracing glacier wastage in the Northern Tien Shan (Kyrgyzstan/Central Asia) over the last 40 years, Climatic Change, 86, 227–234, https://doi.org/10.1007/s10584-007-9288-6, 2008.

Ponomarenko, P. N.: Atmospheric precipitation of Kyrgyzstan, Hydrometeo Publ. House, Leningrad, 134 pp., 1976.

Quincey, D. J., Richardson, S. D., Luckman, A., Lucas, R. M., Reynolds, J. M., Hambrey, M. J., and Glasser, N. F.: Early recognition of glacial lake hazards in the Himalaya using remote sensing datasets, Glob. Planet. Change, 56, 137–152, 2007.

Shatravin, V. I., and Stavisski, J. S.: Methodological bases for the identification of settling factors during detailed studies of high-altitude lakes, Selevye Potoki, Hydrometeolog. Publ. House, 83–92, 1984.

Shatravin, V. I.: Reconstruction of Pleistocene and Holocene glaciations in the Tien-Shan from new starting positions, in: Climate, Glaciers and Lakes: Journey to the Past, Ilim, Bishkek, 26–46, 2007.

Sandwell, D. T., Myer, D., Mellors, R., Shimada, M., Brooks, B., and Foster, J.: Accuracy and resolution of ALOS interferometry: Vector deformation maps of the Father's Day intrusion at Kilauea, IEEE Trans. Geosci. Remote Sens., 46, 3524–3534, https://doi.org/10.1109/TGRS.2008.2000634, 2008.

Strozzi, T., Kääb, A., and Frauenfelder, R.: Detecting and quantifying mountain permafrost creep from in situ inventory, space-borne radar interferometry and airborne digital photogrammetry, Int. J. Remote Sens., 25, 2919–2931, https://doi.org/10.1080/0143116042000192330, 2004.

Usubaliev, R., and Erokhin, S.: Formation of high-mountainous lakes as a consequence of the degradation of the modern glaciation of the Tien Shan, in: Data of Glaciological Studies, NAS KR, Bishkek, 134–137, 2007.

Werner, C., Wegmüller, U., Strozzi, T., and Wiesmann, A.: Gamma SAR and interferometric processing software, in: Sawaya-Lacoste, H. (Ed.), ERS-ENVISAT Symp., Gothenburg, Sweden, ESA Publ. Div., Noordwijk, 2000.

Yamada, T.: Glacier lake and its outburst flood in the Nepal Himalaya, Data Center for Glacier Research, Japanese Society of Snow and Ice, Monograph No. 1, Tokyo, 1998.

Zaginaev, V., Ballesteros-Cánovas, J., Matov, E., Petrakov, D., and Stoffel, M.: Reconstruction of glacial lake outburst floods in northern Tien-Shan: Implications for hazard assessment, Geomorphology, 269, 75–84, https://doi.org/10.1016/j.geomorph.2016.06.028, 2016.

Zaginaev, V., Falatkova, K., Jansky, B., Sobr, M., and Erokhin, S.: Development of a potentially hazardous pro-glacial lake in Aksay valley, Kyrgyz Range, northern Tien Shan, Hydrology, 6, 3, https://doi.org/10.3390/hydrology6010003, 2019.

Zhang, T., Wang, W., An, B., and Wei, L.: Enhanced glacial lake activity threatens numerous communities and infrastructure in the Third Pole, Nat. Commun., 14, 8250, https://doi.org/10.1038/s41467-023-44123-z, 2023.